

# Analysis of Bacterial Migration: II. Studies with Multiple Attractant Gradients

Ian Strauss, Paul D. Frymier, Christopher M. Hahn, and Roseanne M. Ford  
Dept. of Chemical Engineering, University of Virginia, Charlottesville, VA 22903

*Many motile bacteria exhibit chemotaxis, the ability to bias their random motion toward or away from increasing concentrations of chemical substances which benefit or inhibit their survival, respectively. Since bacteria encounter numerous chemical concentration gradients simultaneously in natural surroundings, it is necessary to know quantitatively how a bacterial population responds in the presence of more than one chemical stimulus to develop predictive mathematical models describing bacterial migration in natural systems. This work evaluates three hypothetical models describing the integration of chemical signals from multiple stimuli: high sensitivity, maximum signal, and simple additivity. An expression for the tumbling probability for individual stimuli (Brown and Berg, 1974) is modified according to the proposed models and incorporated into the cell balance equation for a 1-D attractant gradient (Ford and Cummings, 1992). Random motility and chemotactic sensitivity coefficients, required input parameters for the model, are measured for single stimulus responses. Theoretical predictions with the three signal integration models are compared to the net chemotactic response of *Escherichia coli* to co- and antidirectional gradients of D-fucose and  $\alpha$ -methylaspartate in the stopped-flow diffusion chamber assay. Results eliminate the high-sensitivity model and favor the simple additivity over the maximum signal. None of the simple models, however, accurately predict the observed behavior, suggesting a more complex model with more steps in the signal processing mechanism is required to predict responses to multiple stimuli.*

## Introduction

### Chemotaxis

Bacteria in their natural habitats are continually exposed to changing environmental conditions. Their survival depends on their capacity to respond favorably to adverse circumstances. Motile bacteria can respond by moving to a more desirable environment. They are attracted toward chemicals which are beneficial to them (sugars and amino acids) and repelled by chemicals which are either toxic to them (alcohols) or indicators of unfavorable conditions (metabolites). This behavior, known as chemotaxis, plays a critical role in the distribution and dynamic interaction of bacterial populations associated with many microbial processes (Chet and Mitchell, 1976) such as pathogenesis of infection (Freter et al., 1979, 1981), nitrogen fixation (Armitage et al., 1988; Gulash et al., 1984), denitrification (Kennedy and Lawless, 1985), the development of

biofilms (Chet and Mitchell, 1976; Gristina, 1987), and the biodegradation of groundwater contaminants (Bosma et al., 1988; Corapcioglu and Haridas, 1985; Harvey, 1991).

The observed macroscopic behavior involving bacterial population migration is a consequence of the swimming behavior exhibited by individual bacteria at the microscopic level. The paths that individual flagellar bacteria trace as they swim through the surrounding medium are described as a series of relatively straight line "runs" followed by "tumbles" which usually result in a change in orientation (Berg and Brown, 1972; Macnab and Koshland, 1972; Spudich and Koshland, 1975). Typical swimming speeds are 20–60  $\mu\text{m/s}$  (Macnab and Aizawa, 1984) with runs lasting up to several seconds and tumbles taking about a tenth of a second. In an isotropic medium, the swimming behavior resembles a three-dimensional (3-D) random walk analogous to molecular diffusion. In molecular diffusion, however, a change in direction results from a collision with another molecule, while for bacteria a

Correspondence concerning this article should be addressed to R. M. Ford.

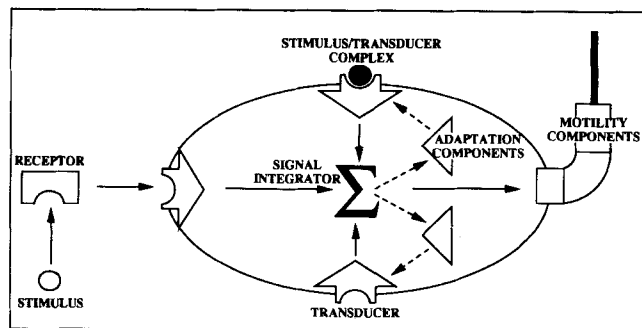


**Figure 1. Information flow through the bacterial chemosensory system of *E. coli*.**

Solid arrows follow the stimulus-receptor interactions from the periplasmic region to the flagellar motor; dashed arrows indicate the feedback control mechanism (Stewart and Dalquist, 1987).

change in direction results from a reversal of flagellar rotation from counterclockwise to clockwise. In the presence of an attractant gradient, a cell is able to decrease its tumbling frequency (increase its run time) if it is moving in a favorable direction and thereby is biasing its random walk to achieve net migration toward higher attractant concentrations.

### Chemosensory mechanism

As bacteria move about exploring their surroundings, they monitor changes in chemical concentrations through special proteins called receptors located near the cell surface. These receptors, like enzymes, have specific binding sites to which only a narrow range of structurally-similar chemical substrates can bind. It is the change in the number of bound receptors over time that provides information to the cell regarding chemical gradients (Macnab and Koshland, 1972). This interaction generates a biochemical signal which controls the flagellar rotation and hence the "decision" whether to tumble or to continue swimming. Although the biochemical pathway for communicating concentration gradient information to the flagellar motors—in particular, signal integration and regulation—is not completely understood, the primary steps in the pathway are well-known from studies of nonchemotactic mutants of *E. coli* and *S. typhimurium*. The initial steps in the pathway, as illustrated by Stewart and Dalquist (1987), are shown in Figure 1. Recent reviews of the signal transduction mechanism include those by Stock et al. (1989) and Eisenbach (1991). Four methyl-accepting chemotaxis proteins (MCPs) have been identified in *E. coli* which act as chemotactic signal transducers: Tsr (taxis to serine and from repellents), Tar (taxis to aspartate and from repellents), Trg (taxis to ribose and galactose), and Tap (taxis associated protein) for dipeptides. These transmembrane proteins convey information from the environment across the cytoplasmic membrane to the interior of the cell. Located on the periplasmic side of the transducer proteins are specific binding sites for chemoattractants and repellents. Amino acids such as serine and aspartate bind directly to Tsr and Tar, respectively, while sugars such as ribose and galactose bind first to periplasmic binding proteins which then interact with Trg. The binding event on the periplasmic portion of the transducer induces a structural change on the cytoplasmic side which initiates a cascade of phosphorylation

reactions involving proteins encoded from CheA and CheY. Phosphorylated CheY protein interacts with the flagellar motors to control the reversal mechanism. The cytoplasmic portion of the transducer also has several reversible methylation sites which are important in adaptation (Stock and Stock, 1987).

### Multiple stimuli

Several investigators have studied bacterial chemotactic responses in the presence of multiple stimuli (Adler and Tso, 1974; Mowbray and Koshland, 1987; Rubik and Koshland, 1978; Tsang et al., 1973). Using the temporal gradient apparatus, Tsang et al. (1973) exposed *Salmonella typhimurium* LT2 to rapid concentration changes from one uniform spatial environment to another. Bacteria which experienced a sudden decrease in phenol (a repellent) concentration exhibited a smooth swimming response (running without tumbling) for an extended period of time before gradually returning to their normal tumbling frequency. They observed that the duration of this smooth swimming response could be progressively reduced by superimposing an opposing stimulus of increasing strength such as an increase in acetate (a repellent) concentration or a decrease in serine (an attractant) concentration. When the second stimulus was large enough, a tumbling response resulted instead of a smooth swimming response, which they concluded was consistent with the idea of algebraically additive stimuli converging to a common pathway. In order to distinguish between the response being merely a statistical average (in which bacteria follow the attractant part of the time and the repellent another part of the time) and being an actual integration of information processed from both stimuli simultaneously, Adler and Tso (1974) observed the rotation of *E. coli* AW607 cells tethered to a glass slide in conflict situations involving aspartate (an attractant) and valine (a repellent). Counterclockwise rotation corresponds to smooth swimming and clockwise rotation to tumbling. They concluded that one stimulus did not dominate over the other and that bacteria do indeed process both signals and bias their response to whichever is present in the more effective concentration. Studies of response recovery time in temporal gradient assays by Rubik and Koshland (1978) revealed that the response of *S. typhimurium* to two simultaneous stimuli is not necessarily additive. When exposed to two different types of attractants, L-aspartate and D-ribose, the response recovery time of the wild type LT2 strain to the combination of stimuli was found to be smaller than the sum of the individual recovery times. The ST171 mutant strain, however, showed exact additivity in the recovery times when exposed to an amino acid and a sugar. For other mutants such as ST313, the recovery time was found to be greater than the sum of the individual stimuli responses. Aspartate and maltose gradients are both sensed through the same MCP and appear to be uncoupled and additive in the response they elicit in *E. coli* (Mowbray and Koshland, 1987). Mowbray and Koshland (1987) found that the response of *E. coli* to aspartate and maltose was slightly less than the sum of the two individual responses but greater than each individual response based on the response times measured in a tethering assay. All of the above mentioned studies were directed toward elucidating the biochemical pathways involved in signal transduction and consequently did not measure parameters which

could be used directly in mathematical models for predicting the migration behavior of bacterial populations.

One investigation aimed toward developing a mathematical model for predicting bacterial population migration in the presence of multiple chemical gradients was reported by Boon and Herpigny (1986). Experimental observations of the combined response to simultaneous gradients of oxygen and glucose involved three different initial configurations for comparison to their model. Based on a macroscopic approach using the Keller and Segel flux expression (Keller and Segel, 1971) their model included terms for random motility and chemotaxis. However, their expression for the chemotactic velocity had no explicit relation to the fundamental binding events involved in chemotaxis. This contrasts our microscopic approach which incorporates receptor binding events that affect the tumbling probabilities associated with individual cell swimming behavior. Although their model provided good qualitative agreement with experimentally observed bacterial density profiles in terms of the numbers of bands that formed, the direction of band migration and the relative position of the bands with respect to the concentration gradients, it relied on several fitting parameters. If the random motility and the chemotactic responses to oxygen and glucose had been measured independently first, then the number of parameters determined by fitting would have been reduced. For this reason, a mathematical model based on the underlying mechanisms by which bacteria integrate their response to multiple stimuli is desirable.

The mathematical model used in the analysis of our experimental results is based on a simple mechanism which assumes equilibrium binding of attractant to the periplasmic receptors and a direct correspondence between the number of bound receptors and the chemotactic signal. This mechanism has been shown to adequately describe experimentally observed chemotactic responses for single stimuli (Ford et al., 1991). Bray and co-workers (1993) provide a more detailed mathematical description of the chemosensory mechanism accounting for the kinetics associated with each step in the pathway. However, their model does not include a mechanism for adaptation (which is implicit in the simple model we employ) and thus is limited in its application to short-term responses of bacteria. In addition, their signal transduction model has not been incorporated into cell balance equations to describe the migration of bacterial populations. Consequently, this model will not be considered further in this article.

## Experimental Methods

Our experimental system, *E. coli*/fucose/ $\alpha$ -methylaspartate, represents two attractants which utilize different MCPs for signal transduction. Fucose is a structural analog of galactose which binds to the galactose-binding protein although with a lower affinity than galactose (Adler, 1969). This complex then binds to the Trg MCP to initiate the chemotactic signal. Because *E. coli* are not capable of metabolizing fucose (Adler, 1969), complications in our chemotaxis assay associated with oxygen consumption during metabolism and the development of secondary chemotactic responses to oxygen gradients are eliminated. The selection of  $\alpha$ -methylaspartate as the second attractant was for similar reasons. Although  $\alpha$ -methylaspartate is not metabolized by *E. coli*, it does bind to the Tar MCP

because it is similar in structure to aspartate (Adler and Tso, 1974; Mesibov et al., 1973).

## Growth conditions

A loopful of *E. coli* K12 (NR50) cells was scraped from a frozen stock and used to inoculate 25 mL of minimal media (Adler and Dahl, 1967) which was supplemented with 1 mL of 0.5 mg/mL thiamine and 0.1-g/mL D-galactose per 100 mL prior to inoculation. Galactose was used as the limiting substrate during growth in order to induce the production of galactose-binding proteins necessary for a response to fucose in the chemotaxis assay. Aspartate is not required in the growth medium because the Tar protein is produced constitutively. The culture, contained in a 250 mL shake flask, was grown for 17 h at 30°C on a rotary shaker set at 150 rpm. A 12-mL aliquot of bacteria was removed and gently washed using a filtering technique similar to Berg and Turner (1990) to avoid shearing off the flagella. The bacteria were then resuspended to a density of  $10^9$  cells/mL in motility buffer (Adler and Templeton, 1967) which had been filtered through 0.22  $\mu$ m filter paper to remove debris. Motility buffer was supplemented with 1.0-g polyvinylpyrrolidone (PVP-40) per liter of distilled water to reduce adhesion of bacteria to the glass slides (Berg and Turner, 1990). Strauss (1992) provides further details related to preparation of the bacteria.

## Stopped-flow diffusion chamber assay

The stopped-flow diffusion chamber (SFDC) assay shown in Figure 2 is advantageous for the study of bacterial chemotaxis, because it provides well-characterized chemical gradients (Ford and Lauffenburger, 1991b; Ford et al., 1991). The fluid flow behavior within the chamber involves the contact of two suspensions by impinging flow. One critical aspect is that while the fluid is flowing no mixing occurs between the two suspensions and a step change in stimulus concentration can be maintained to establish well-defined initial conditions.

The random motility coefficient was determined in the absence of a chemical gradient. A bacterial suspension consisting of a 1-mL aliquot of resuspended culture per 99 mL of motility buffer was divided into two equal portions. The first portion was filtered through a 0.45  $\mu$ m syringe filter to remove the bacteria and added to 0.25-mL Percoll (colloidal PVP coated silica, Sigma P1644) to make up 50 mL of solution. Percoll was added to increase the density in the lower half by a small amount in order to prevent density-driven convection. This solution was then pumped into the base of the chamber with the second portion simultaneously entering from the top. During flow a sharp step change in bacterial density was maintained between the two halves of the chamber. When the flow was stopped, bacteria in the upper half of the chamber began swimming into the lower half and the initial step change in bacterial density gradually decayed with time.

Chemotaxis experiments were performed in the same manner as the random motility experiments except in the presence of an attractant gradient. The bacterial suspension entering the top region of the chamber was prepared in the same way as described above. The suspension in the bottom of the chamber contained 0.125-mL Percoll, 0.25-mL culture and the required amount of chemoattractant per 25 mL of motility buffer. For single stimulus experiments with  $\alpha$ -methylaspartate,  $\alpha$ -methyl-

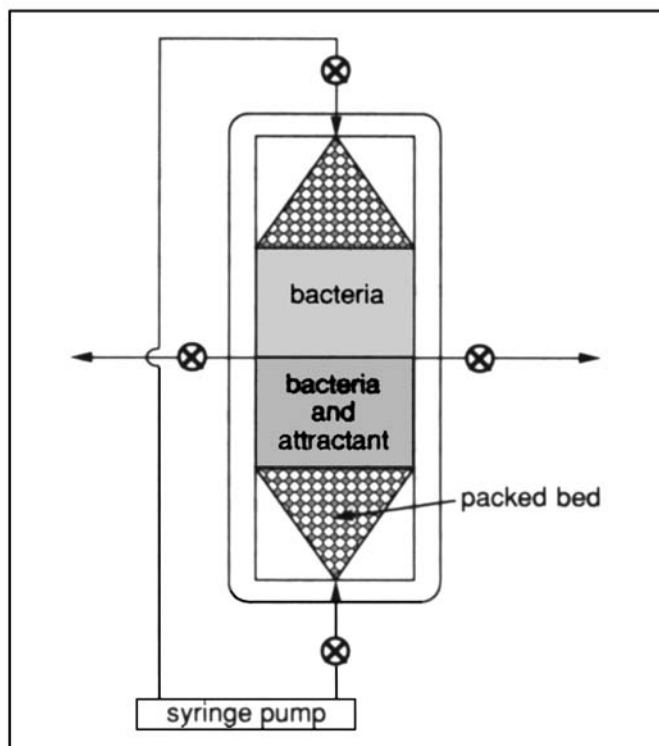


**Figure 2. SFDC with two glass microscope slides with a 0.19 mm gap between them form the walls of the chamber.**

Fluid enters the chamber through 0.6 mm slits in the top and bottom and exits through similar slits on either side directly across from each other and perpendicular to the centerline connecting the top and bottom slits. Three-way valves at each of the four openings are used to control flow to and from the chamber. Triangular-shaped packed beds help to dissipate the momentum of the incoming fluid and evenly distribute flow across the width of the chamber.

DL-aspartic acid (Sigma M6001) was used at a concentration of 0.01 mM. (Data for the single stimulus experiments with 0.1 mM fucose were obtained from previously reported results in Ford et al. (1991).) To determine the effects of multiple stimuli, a mixture of  $\alpha$ -methylaspartate and D-fucose (Sigma F2127) was used at concentrations of 0.01 mM and 0.032 mM, respectively. The experimental concentrations were selected to avoid complications in the experiments that resulted from high concentrations and yet still produce single stimulus responses that were well within the detection limits of the SFDC assay. The  $\alpha$ -methylaspartate concentration used was the highest concentration for which a second chemotactic band did not appear. The formation of a second band was presumably due to a secondary low affinity receptor that produced a response at high concentrations (Dahlquist et al., 1972; Ford and Laufenburger, 1991a; Segel, 1977). The appropriate fucose concentration was chosen by increasing above the benchmark of the  $\alpha$ -methylaspartate concentration to the point at which a significant chemotactic response was observed for fucose in the single stimulus assay.

Initially, while the solutions were flowing through the chamber, the bacterial density remained uniform throughout the chamber and a step change in attractant concentration was maintained between the upper and lower halves. The various configurations including the cases for co- and antidirectional

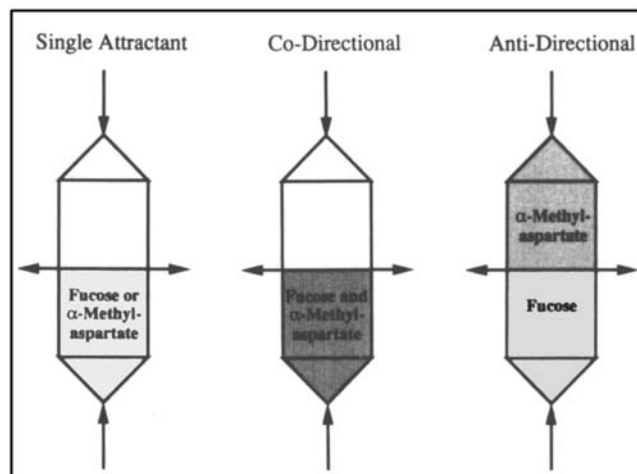


**Figure 3. Attractant gradient configurations for chemotaxis experiments in the SFDC.**

The initial bacterial density is uniform throughout the entire chamber.

gradients which were used in experiments are shown in Figure 3. In the single attractant configuration, when flow was stopped attractant in the bottom half began to diffuse into the upper half setting up a transient gradient in the attractant concentration. As bacteria sensed and responded to this gradient, a band of high cell density formed immediately and moved downward toward higher attractant concentrations as time progressed and the attractant gradient decayed. Similar behavior was observed for the co-directional configuration with a more highly visible band. In the antidirectional configuration the chemotactic band moved toward the  $\alpha$ -methylaspartate.

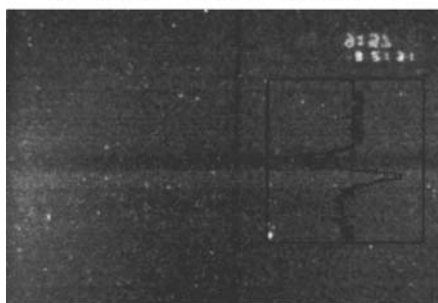
Light scattering was used to detect changes in bacterial density within the SFDC. The chamber was illuminated from behind by a Schott model KL1500 light source fitted with a heat filter and two light guide extensions. A green interference filter was placed behind the heat filter to provide the best contrast levels for black and white photography. The two light guides were positioned on either side of the chamber so that light struck the chamber at an angle of 45°. In the chamber, regions of high bacterial density appeared light and regions of low bacterial density appeared dark. For dilute bacterial suspensions such as those used in our experiments the amount of scattered light detected by the camera was assumed to be linearly proportional to the number density of bacteria.

The microscope was fitted with a phototube to which a Contax 35 mm camera was attached. Photographs were taken at periodic time intervals to record the bacterial density distributions. Black and white images were recorded on Kodak Tmax P3200 film at an exposure time of 1 s.

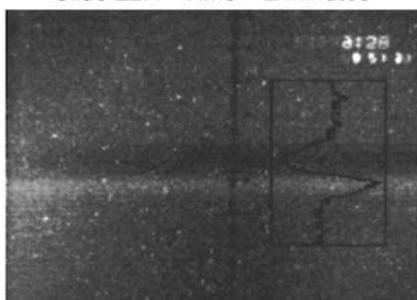
### Image analysis

Bacterial density distribution profiles within the chamber were obtained by computer-aided image analysis of negatives of the photographs using equipment and software made available to us through the Image Processing Center at the University of Virginia. Each negative was scanned by an Eikonix 78/99 Image Digitizer through a 55 mm Nikon lens and two 36-mm and 11-mm extensions (total magnification = 2.8 ×).

Slide 22.2 Time = 30 seconds



Slide 22.4 Time = 2 minutes



Slide 22.6 Time = 7 minutes

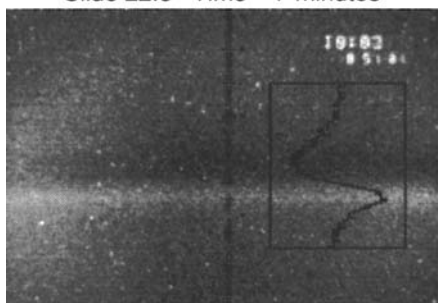


**Figure 4. Digitized images from a chemotaxis experiment in the SFDC for the response of *E. coli* to an initial concentration of 0.01 mM  $\alpha$ -methylaspartate at three experimental times.**

Light band is the result of a higher bacterial density reflecting net migration toward the attractant. Superimposed graph shows the bacterial density computed from gray level measurements averaged over the region indicated by the rectangle.

The digitizer divides each image into an array of  $512 \times 512$  pixels. Each pixel is assigned a gray level ranging from 0 to 255 based on the light intensity measured by a photodiode at the corresponding point on the original image. A gray level of 255 corresponds to the darkest setting for which no light reaches the photodiode. Image files acquired on the Eikonix Digitizer were stored on a  $\mu$ VAX computer and later downloaded for analysis using Image 1.41 (Wayne Rasband, National Institutes of Health). Rectangular regions of the digitized image were selected for analysis with the image processing software and scanned horizontally at approximately 100 positions. The image processor generated vertical gray-level profiles by horizontally averaging the gray levels across the image. Examples of the digitized images with the profiles superimposed are shown in Figure 4. Pixels were calibrated to distance in units of cm through a reticule in the eyepiece of the microscope that appeared on each negative. Bacterial density was calibrated to

brated to gray levels using a linear relationship based on two known densities from the random motility experiments. This linear relationship was only valid for gray level values above 90 (Strauss, 1992). Therefore, in the analysis of our experimental results we used the regions of the bacterial density profiles which corresponded to the lower bacterial densities (gray levels above 90) to avoid the nonlinear regions of the calibration curve. Bacterial density profiles as a function of vertical position in the chamber were then used to determine cell migration properties.

### Mathematical model

The migration of chemotactic bacteria in the SFDC assay was modeled using the cell balance equation for 1-D attractant gradients derived by Ford and Cummings (1992) as a special case of the more general balance equation of Alt (1980). The numerical solution of this balance equation by finite element methods was described in the first article in this series (Frymier et al., 1994). In this section we briefly outline our model equations including the proposed tumbling probability expressions for multiple stimuli.

### Balance equations

The 3-D cell balance equation of Alt (1980) was simplified by Ford and Cummings (1992) for the migration of bacteria in 1-D attractant gradients. Since the chemical attractant gradient is present in one direction only (the  $z$  direction) the cell density is symmetric in the  $x$  and  $y$  directions. Integration over the  $x$  and  $y$  coordinates of position yielded the following balance equation for the bacterial distribution  $n_z$  as a function of position  $z$ , direction angle with respect to the  $z$ -axis  $\theta$ , and time  $t$ :

$$\frac{\partial n_z(z, \theta, t)}{\partial t} = -s_z \frac{\partial v(z, t) n_z(z, \theta, t)}{\partial z} - \beta(z, \theta, t) n_z(z, \theta, t) + \int_0^\pi \beta(z, \theta', t) n_z(z, \theta', t) K(\theta', \theta) \sin \theta' d\theta' \quad (1)$$

where  $v(z, t)$  is the mean swimming speed,  $s_z$  is the  $z$ -component of the unit direction vector,  $\beta(z, \theta, t)$  is the tumbling probability (whose functional form is described below) and  $K(\theta', \theta)$  is the probability per unit angular measurement that a bacterium moving in a direction at angle  $\theta'$  to the  $z$ -axis will change direction after tumbling to angle  $\theta$  with respect to the  $z$ -axis. Equation 1 physically represents the time rate of change in the number density of bacteria  $n_z(z, \theta, t)$  resulting from losses due to convective motion away from the point  $z$  and due to tumbling with a probability density  $\beta(z, \theta, t)$  and a gain due to bacteria moving in direction  $\theta'$  which tumbled and began moving in the direction  $\theta$ . For the conditions associated with the SFDC assay, bacterial growth and death are negligible.

The quantity which corresponds to the bacterial density that is measured experimentally  $c(z, t)$  is related to the angle dependent density  $n_z(z, \theta, t)$  by:

$$c(z, t) = \int_0^\pi n_z(z, \theta, t) \sin \theta d\theta \quad (2)$$

The attractant concentration profile follows the familiar diffusion equation:

$$\frac{\partial a}{\partial t} = D \frac{\partial^2 a}{\partial z^2} \quad (3)$$

with diffusion coefficient  $D$ . Note that a consumption term is not required in this equation because the attractants are not metabolized. The maximum specific uptake rate for fucose is essentially zero (Ford and Lauffenburger, 1991b) and although it has not been reported for  $\alpha$ -methylaspartate (Mesibov et al., 1973) uptake has been neglected in similar studies (Brown and Berg, 1974). For the boundary and initial conditions associated with the experimental assay used in this work the solution of Eq. 3 is given by:

$$a(z, t) = \frac{a_0}{2} \left[ 1 + \operatorname{erf} \left( \frac{z}{\sqrt{4Dt}} \right) \right] \quad (4)$$

### Tumbling probability models

A general equation describing the tumbling probability  $\beta(z, \theta, t)$  in the presence of a 1-D attractant gradient for a single attractant is given by:

$$\beta(z, \theta, t) = \begin{cases} \beta_0 \exp(-\epsilon), & \epsilon > 0 \\ \beta_0, & \epsilon < 0 \end{cases} \quad (5)$$

where  $\beta_0$  is the experimentally measured tumbling probability in the absence of a chemical gradient (Frymier et al., 1993, 1994; Rivero et al., 1989). Equation 5 assumes a Poisson process for tumbling and incorporates the observation by Berg and Brown (1972) in which the tumbling probability for *E. coli* returns to  $\beta_0$  when moving down-gradient. The argument of the exponential, defined by:

$$\epsilon = \frac{\chi_0^{3D}}{\nu} \frac{K_d}{(K_d + a)^2} \cos \theta \frac{\partial a}{\partial z} \quad (6)$$

represents the chemotactic signal—a combination of the chemotactic sensitivity coefficient  $\chi_0$  and the spatial attractant gradient—with dissociation constant  $K_d$  for the attractant-receptor binding equilibrium. The functional form of the expression for the chemotactic signal is based on tracking experiments of *E. coli* reported by Brown and Berg (1974). The random motility coefficient  $\mu_0$  is related to  $\beta_0$  according to (Lovely and Dalquist, 1975):

$$\mu_0 = \frac{\nu^2}{3\beta_0(1-\psi)} \quad (7)$$

where  $\psi$  is a persistence parameter estimated from the Brown and Berg data to be 0.36 for *E. coli*.

We consider three hypothetical models for the tumbling probability  $\beta(z, \theta, t)$  in the presence of multiple stimuli: (1) Response only to the attractant present with the highest chemotactic sensitivity  $\chi_0$ ; (2) response to the maximum individual chemotactic signal  $\epsilon$  at any one time; and (3) response pro-

portional to simple additivity of individual chemotactic signals,  $\Sigma \epsilon_i$ . These models can be compared with mixture rules used in thermodynamics to predict thermophysical properties of fluid mixtures based on measurements of the properties for pure substances (Sandler, 1977). In our experimental system, the first model, “high sensitivity,” would use the tumbling probability equation for a single attractant (Eq. 5) with parameter values for  $\alpha$ -methylaspartate, because the chemotactic sensitivity of  $\alpha$ -methylaspartate is significantly higher than that for fucose. This model implies that the chemotactic response is controlled by a single attractant which dominates signaling for the bacteria and all other attractants with smaller  $\chi_0$  are ignored. The second model, “maximum signal,” is based on the hypothesis that the bacteria respond to the strongest chemotactic signal which combines both the chemotactic sensitivity and the strength of the gradient. This differs from the high-sensitivity model, because bacteria will respond to a fucose signal in the presence of  $\alpha$ -methylaspartate if the fucose gradient is large enough to compensate for a lower chemotactic sensitivity coefficient. In terms of the tumbling probability, this model is defined by:

$$\beta(z, \theta, t) = \begin{cases} \beta_0 \exp[-\max(\epsilon_i)], & \max(\epsilon_i) > 0 \\ \beta_0, & \max(\epsilon_i) < 0 \end{cases} \quad (8)$$

The third model, “simple additivity,” implies that the responses are additive and independent as suggested by Rubik and Koshland (1978) for *S. typhimurium* ST171/aspartate/serine and *S. typhimurium* ST171/aspartate/ribose. The tumbling probability equation for this model is written as:

$$\beta(z, \theta, t) = \begin{cases} \beta_0 \exp \left[ \sum_i (-\epsilon_i) \right], & \sum_i (-\epsilon_i) > 0 \\ \beta_0, & \sum_i (-\epsilon_i) < 0 \end{cases} \quad (9)$$

## Results

The transport coefficients are determined from analysis of bacterial density profiles observed in the SFDC assay using the mathematical model described above. The results from this analysis are presented in this section.

### Random motility coefficient

The random motility coefficient  $\mu_0$  is determined from an independent experiment performed in the SFDC assay in the absence of a chemical gradient as described in the Experimental Methods section earlier. Under these conditions the cell density  $c$  is well characterized by the diffusion equation:

$$\frac{\partial c}{\partial t} = \mu_0 \frac{\partial^2 c}{\partial z^2} \quad (10)$$

with  $\mu_0$  analogous to a molecular diffusion coefficient. In our experimental configuration the positive  $z$  axis points downward from the center of the chamber. Therefore, the solution of Eq. 10 for bacteria initially in the upper half of the SFDC takes the form of Eq. 4 with a change in the sign preceding the error function. To relate the solution of Eq. 10 to our

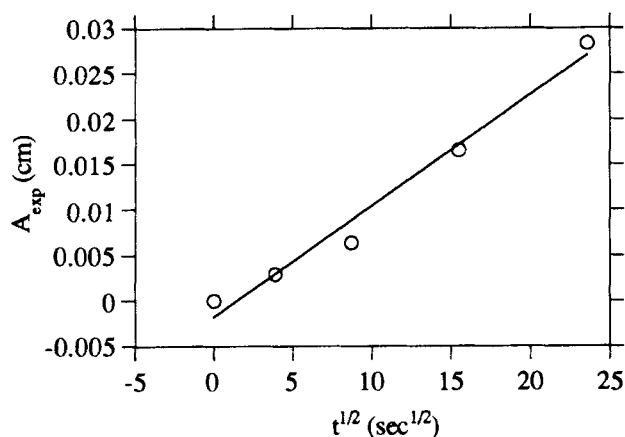


**Figure 5. Experimental accumulation  $A_{\text{exp}}$  which corresponds to  $N(t)/A_x$  as a function of  $t^{1/2}$  from a random motility experiment.**

A linear regression analysis of the data produced the solid line shown in the graph with a slope of  $0.00122 \text{ cm/s}^{1/2}$  and a correlation factor  $r$  equal to 0.98952. The resulting random motility coefficient is  $(4.7 \pm 0.8) \times 10^{-6} \text{ cm}^2/\text{s}$ .

experimental profiles we integrate the bacterial density profile over the bottom half of the chamber which corresponds to the number of bacteria  $N(t)$  that have moved across the interface per unit cross-sectional area of the chamber  $A_x$ . The random motility coefficient  $\mu_0$  is then determined from the following relationship:

$$\frac{N(t)}{A_x} = \int_0^{L/2} c(z, t) dz = c_0 \sqrt{\frac{\mu_0 t}{\pi}} = A_{\text{exp}} \quad (11)$$

where  $L$  is the total length of the chamber and  $A_{\text{exp}}$  is the

experimental accumulation of bacteria determined from the area under the curve of bacterial density vs. position and therefore has units of cells/length<sup>2</sup>. When  $A_{\text{exp}}$  is plotted as a function of the square root of time as shown in Figure 5,  $\mu_0$  can be calculated from the slope of the line  $m$  according to  $\mu_0 = \pi \cdot m^2$ . (See Ford et al. (1991) and Mercer et al. (1993) for details of the analysis.) Values for the random motility coefficients which were experimentally determined and subsequently used in the theoretical calculations are recorded in Table 1.

### Chemotactic sensitivity coefficient

For the chemotaxis experiments the experimental accumulation  $A_{\text{exp}}$ , which represents the net increase in number of bacteria  $N(t)$  per unit cross-sectional area of the chamber over the initial bacterial density, was used as a measure of the chemotactic response. This accumulation, which corresponds to the area under the peak (or above the trough) in the bacterial density profiles, has been shown to be linearly proportional to  $t^{1/2}$  for chemotactic responses to single stimulus gradients (Ford and Lauffenburger, 1991b; Staffeld et al., 1987). To avoid complications with nonlinearities in the calibration between bacterial density and gray levels associated with high bacterial densities, the depleted region of bacterial density corresponding to the trough was used in our analysis. The chemotactic sensitivity coefficient  $\chi_0$  was determined by matching the experimental slope from a plot of trough area vs.  $t^{1/2}$  with the slope from theoretical bacterial density profiles generated for a range of  $\chi_0$  values. An example of the experimental data with fucose as the attractant is shown in Figure 6. The slope of the line determined by a linear least-squares regression is superimposed on the experimental data and is equal to the slope resulting from a theoretical calculation with

**Table 1. Input Parameters Including Source References for the Finite Element Solution of the Balance Equation for 1-D Attractant Gradients**

Parameter	Value	Source Ref.
Diffusivity, $D$		
fucose	$6.9 \times 10^{-6} \text{ cm}^2/\text{s}$	Ford et al. (1991)
$\alpha$ -methylaspartate	$8.6 \times 10^{-6} \text{ cm}^2/\text{s}$	Brown and Berg (1974)*
Dissociation Constant, $K_d$		
Fucose	0.08 mM	Hazelbauer and Harayama (1983)
$\alpha$ -methylaspartate	0.125 mM	Mesibov et al. (1973)
Swimming Speed, $v$	22 $\mu\text{m/s}$	Berg and Brown (1972)
Initial Attractant Concentration, $a_0$		
fucose-single	0.1 mM	Ford et al. (1991)
fucose-multiple	0.032 mM	Strauss (1992)
$\alpha$ -methylaspartate-single	0.01 mM	Strauss (1992)
$\alpha$ -methylaspartate-multiple	0.01 mM	Strauss (1992)
Random Motility Coefficient, $\mu_0$		
fucose	$(4.7 \pm 0.8) \times 10^{-6} \text{ cm}^2/\text{s}$	Ford et al. (1991)**
$\alpha$ -methylaspartate	$(8.8 \pm 3.8) \times 10^{-7} \text{ cm}^2/\text{s}$	Strauss (1992)**
multiple gradient	$(5.4 \pm 1.4) \times 10^{-6} \text{ cm}^2/\text{s}$	Strauss (1992)**
Chemotactic Sensitivity Coefficient, $\chi_0$		
fucose	$(3.9 \pm 0.1) \times 10^{-5} \text{ cm}^2/\text{s}$	Ford et al. (1991)**
$\alpha$ -methylaspartate	$(4.1 \pm 0.2) \times 10^{-4} \text{ cm}^2/\text{s}$	Strauss (1992)**

\*Brown and Berg report a value for aspartate ( $8.9 \times 10^{-6} \text{ cm}^2/\text{s}$ ), which we then modified for  $\alpha$ -methylaspartate according to the ratio of the molecular weights to the 1/3 power (Tanford, 1961).

\*\*The source listed refers to the raw experimental data; the analysis of the data is part of this work.

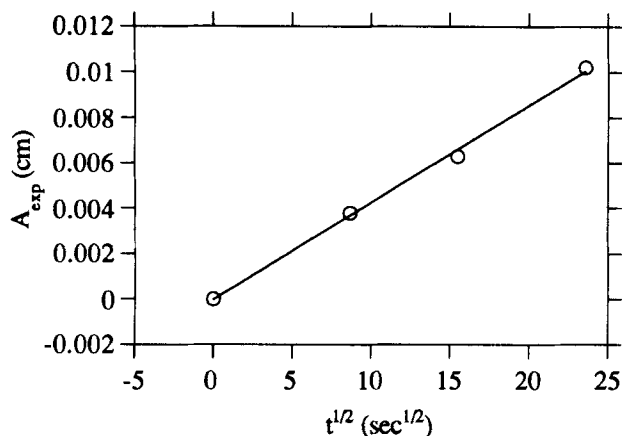


**Figure 6. Bacterial accumulation represented by the trough area as a function of  $t^{1/2}$ .**

The accumulation data are calculated from experimental profiles similar to those in Figure 4 and are from a chemotaxis experiment with an initial attractant concentration of 0.1 mM fucose. A linear regression analysis of the data produced the solid line shown in the graph with a slope of 0.00042866 cm/s<sup>1/2</sup> and a correlation factor  $r$  equal to 0.99877. The chemotactic sensitivity coefficient,  $\chi_0$ , is determined by matching the experimental slope to theoretical predictions over a range of  $\chi_0$  values. For this set of data  $\chi_0 = (3.9 \pm 0.1) \times 10^{-5}$  cm<sup>2</sup>/s.

cm<sup>2</sup>/s. A similar plot for  $\alpha$ -methylaspartate was shown in Frymier et al. (1994). The result from that analysis,  $\chi_0 = 4.1 \times 10^{-4}$  cm<sup>2</sup>/s, is included in Table 1.

Estimates of the errors associated with the above procedure for determining the transport coefficients were based on the correlation coefficients obtained from the linear least-squares regression of the experimental data of  $A_{\text{exp}}$  vs.  $t^{1/2}$ . The standard deviation associated with the slope  $\sigma(m)$  can be determined from the correlation factor  $r$  using the formula (Milton and Arnold, 1990):

$$\sigma(m) \equiv \left[ \frac{1 - r^2}{(N - 2)} \right]^{1/2} \frac{m}{r}$$

with  $N$  data points. Since  $\mu_0$  and  $\chi_0$  (over the range of our experimental data) are linearly proportional to the slope, the fractional error in the transport coefficient is equal to the fractional error in the slope. The standard deviations are reported in Table 1 with the transport coefficients.

### Single stimulus response

Theoretically-generated bacterial density profiles for chemotactic responses to single stimuli based on the finite element solution of Eqs. 1–7 with the parameter values given in Table 1 are compared to experimentally observed profiles in Figure 7 for fucose and Figure 8 for  $\alpha$ -methylaspartate at several experimental times. There is good agreement between the theoretically generated profiles and the experimental observations. Recall that the chemotactic sensitivity coefficient was determined by fitting the trough areas, not by matching the shape of the profiles. The good agreement then suggests that the mechanistic model for the chemotactic response, though relatively simple, provides a reasonable description of a complex bacterial behavior.

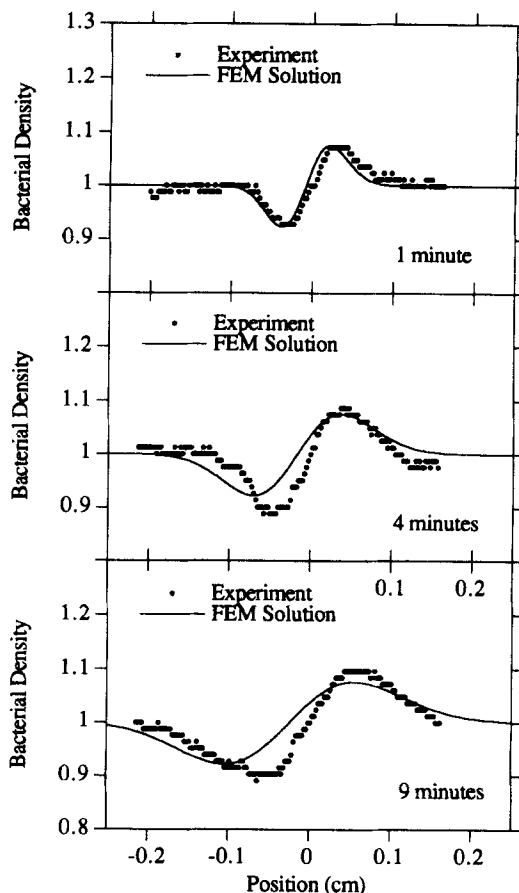


**Figure 7. Bacterial density profiles from the SFDC assay for chemotaxis experiments ( $\circ$ ) with an initial attractant concentration of 0.1 mM fucose at times of 1, 4 and 9 min.**

Fucose was initially present in the bottom of the chamber corresponding to positions greater than zero on the plot. Theoretical profiles (FEM solution) are superimposed with  $\chi_0 = 3.9 \times 10^{-5}$  cm<sup>2</sup>/s (—) for comparison.

### Multiple stimuli response

Our experimentally observed responses of *E. coli* to multiple gradients of fucose and  $\alpha$ -methylaspartate are shown in Figure 9 for the co-directional configuration and in Figure 10 for the antidirectional configuration. From qualitative visual observations during the experiments it appeared that the magnitude of the chemotactic response of the bacteria in the presence of both attractants was much greater than the single stimulus responses to either  $\alpha$ -methylaspartate or fucose. However, it was difficult to compare directly because the random motility of the population for  $\alpha$ -methylaspartate alone was significantly less than that for the multiple stimuli experiment.

We have superimposed on the experimental results for bacterial densities the attractant concentration profiles calculated from Eq. 4 with the appropriate parameter values from Table 1. This was done to illustrate the magnitude of the concentration gradients and the position of the bacterial density peak relative to the attractant concentration profiles. Because the diffusion coefficients for the two attractants differ by less than 25%, the profiles show essentially the same evolution in time. The fucose gradient is 3.2 times steeper than the one for  $\alpha$ -



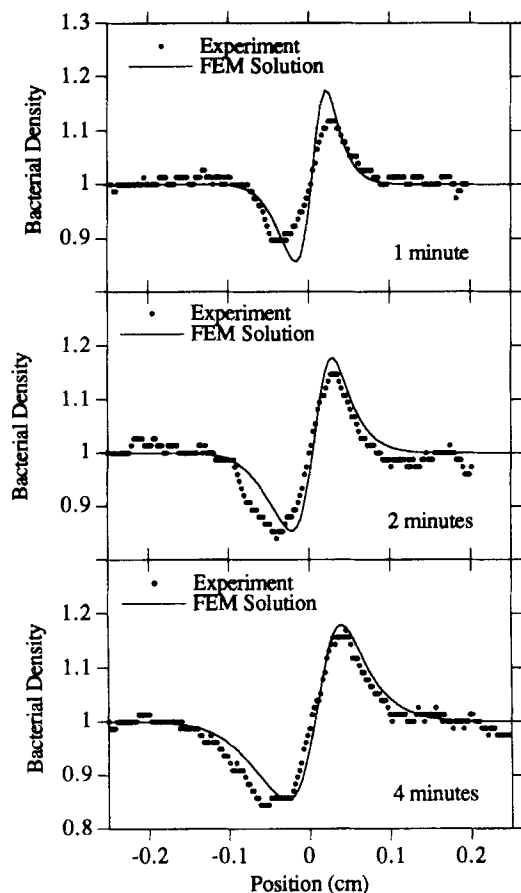


**Figure 8. Bacterial density profiles from the SFDC assay for chemotaxis experiments (○) with an initial attractant concentration of 0.01 mM  $\alpha$ -methylaspartate at times of 1, 2 and 4 min.**

Methylaspartate was initially present in the bottom of the chamber, corresponding to positions to the right of zero on the plot. Theoretical (FEM solution) profiles are superimposed with  $\chi_0 = 4.1 \times 10^{-4} \text{ cm}^2/\text{s}$  (—) for comparison.

methylaspartate. If we compare the gradients relative to the respective dissociation constants which correspond to the concentrations evoking the strongest response, fucose is greater by a factor of 5. However, the bacteria move toward  $\alpha$ -methylaspartate and away from fucose in the antidirectional configuration indicating that the greater chemotactic sensitivity of  $\alpha$ -methylaspartate can more than compensate for a larger fucose gradient.

### Evaluation of proposed models

In general, we cannot directly compare the experimental profiles to evaluate the proposed models because the fucose concentrations were different between the single stimulus and multiple stimuli experiments and the random motility coefficients were different for each of the experiments. Random motility coefficients can vary depending on the growth rate (which is difficult to control in batch culture) and washing technique. Mercer et al. (1993) observed a factor of 5 difference over a range of growth rates ( $0.07\text{--}0.15 \text{ h}^{-1}$ ). However, using the mathematical model we can compare our predictions with any set of experimental conditions.

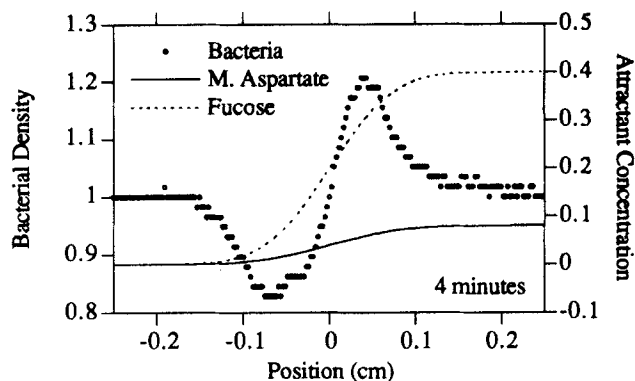


**Figure 9. Bacterial density profiles for multiple stimulus experiments (○) in the co-directional configuration at 4 min.**

Initial attractant concentrations are 0.01 mM  $\alpha$ -methylaspartate and 0.032 mM fucose. Attractant concentration profiles plotted as dimensionless concentration ( $a/K_d$ ) for fucose (---) and  $\alpha$ -methylaspartate (—) are superimposed.

The one direct experimental comparison which can be made is between the results for the co- and antidirectional configurations of the two attractants. For these cases, the fucose concentrations and random motility coefficients are the same. According to the high-sensitivity model, bacteria would only respond to the attractant with the larger chemotactic sensitivity coefficient, in our case  $\alpha$ -methylaspartate. The presence of the less dominant attractant, fucose, would be ignored. We would then expect the bacterial density profiles to be mirror images of each other because the  $\alpha$ -methylaspartate gradient is identical except that it is initiated from opposite sides of the chamber. It is clear from Figures 9 and 10 that the profiles differ significantly and, therefore, we conclude that the high-sensitivity model does not accurately model the multiple gradient response.

Plots of bacterial accumulation (corresponding to the area associated with the trough) vs.  $t^{1/2}$  for the three different tumbling probability models are compared to each other and to the experimental data for the codirectional configuration (Figure 11a) and antidirectional configuration (Figure 11b). The

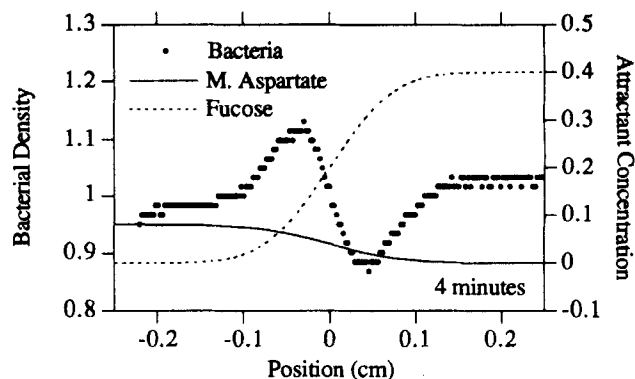


**Figure 10. Bacterial density profiles for multiple stimulus experiments (○) in the antidirectional configuration at 4 min.**

Initial attractant concentrations are 0.01 mM  $\alpha$ -methylaspartate and 0.032 mM fucose; attractant concentration profiles plotted as dimensionless concentration ( $a/K_d$ ) for fucose (---) and  $\alpha$ -methylaspartate (—) are superimposed.

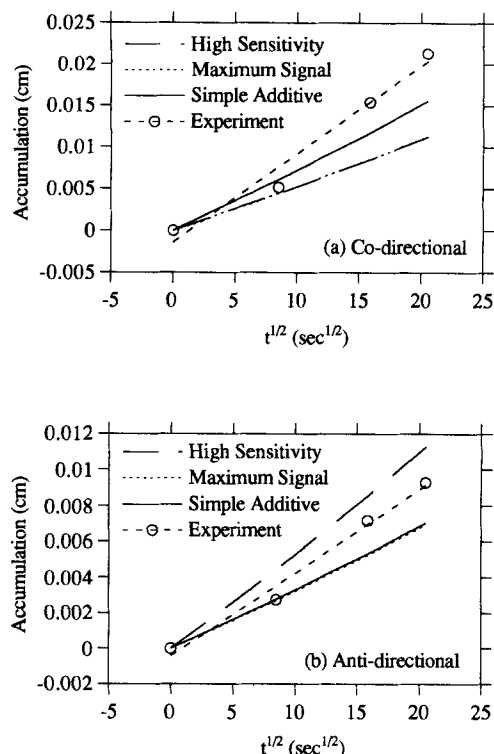


**Figure 11. Accumulation vs.  $t^{1/2}$  plots for multiple stimuli experiments ( $\circ$ ) with an initial attractant concentration of 0.01 mM  $\alpha$ -methylaspartate and 0.032 mM of fucose.**

A linear regression analysis of the experimental data (---) is compared to theoretical predictions based on the high sensitivity (---), maximum signal (---) and simple additivity (—) models for the (a) co-directional configuration and (b) antidirectional configuration. High-sensitivity and maximum signal model predictions are identical and appear as a line with a combination of long and short dashes in (a).

differences in the experimental slopes between the co- and anti-directional configurations imply that the high-sensitivity model is also incorrect for this system. In the co-directional case all the models underpredict the magnitude of the response as indicated by the slope of the line. The slope for the simple additivity model is closer to the experimental result than the slopes for the high-sensitivity and maximum signal models which have the same value. For the antidirectional configuration the maximum signal and simple additivity models yield the same slope which underpredicts the experimental result while the high-sensitivity model overpredicts the experimental slope by roughly the same magnitude.

We also compare theoretical predictions of the bacterial density profiles for the three different tumbling probability models to each other and to the experimental data for the co-directional (Figure 12) and antidirectional (Figure 13) configurations. The comparisons are shown at four min because the differences between the models and the experimental data are more pronounced at this later time. The same qualitative trends were observed at 1 and 2 min.

In assessing the maximum signal model we note that for the co-directional gradients, the  $\alpha$ -methylaspartate signal (as defined by Eq. 6) will always be stronger because of the ten-fold larger chemotactic sensitivity coefficient although the fucose

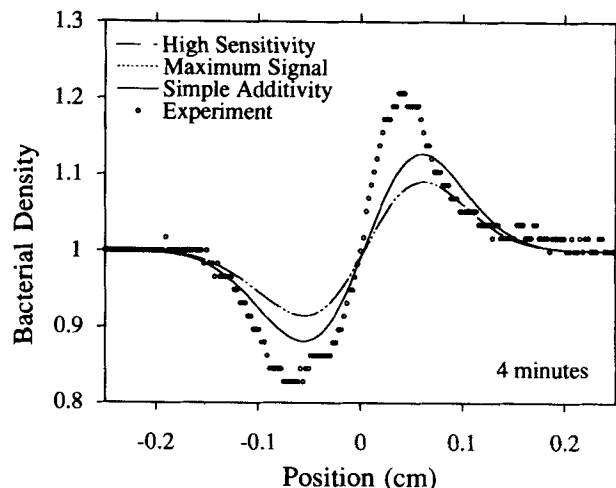


**Figure 12. Bacterial density profiles for multiple stimuli experiments ( $\circ$ ) with an initial attractant concentration of 0.01 mM  $\alpha$ -methylaspartate and 0.032 mM of fucose.**

These are compared to theoretical predictions based on the high sensitivity (---), maximum signal (---) and simple additivity (—) models for the codirectional configuration. The high sensitivity and maximum signal model predictions are identical and appear as a line with a combination of long and short dashes.

gradient is initially steeper by a factor of three. Therefore, in a co-directional configuration we expect predictions of the multiple gradient response to be very similar to the single stimulus response to  $\alpha$ -methylaspartate (and to the high-sensitivity model). Because the maximum signal model is identical to the high-sensitivity model for this configuration it also underpredicts the response to multiple gradients. For the anti-directional configuration, bacteria moving against the  $\alpha$ -meth-

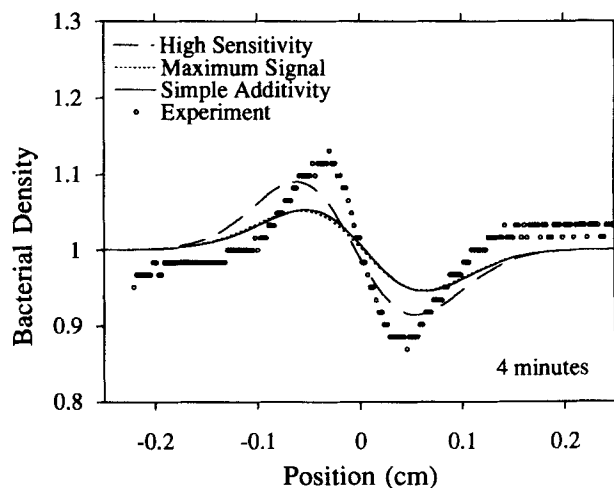


**Figure 13. Bacterial density profiles for multiple stimuli experiments ( $\circ$ ) with an initial attractant concentration of 0.01 mM  $\alpha$ -methylaspartate and 0.032 mM of fucose.**

These are compared to theoretical predictions based on the high sensitivity (---), maximum signal (---) and simple additivity (—) models for the antidirectional configuration.

ylaspartate gradient would respond to the fucose stimulus instead of returning to their basal tumbling frequency. This would increase the run lengths for bacteria moving away from the  $\alpha$ -methylaspartate and tend to reduce the number of bacteria crossing the interface and hence reduce the peak area of the bacterial density profile as compared to the high-sensitivity model and  $\alpha$ -methylaspartate alone. In summary, for the antidirectional configuration the high-sensitivity model agrees more closely with the experimental data than the maximum signal model, but both significantly underpredict the observed response.

The simple additivity model would predict a response to the co-directional gradient equivalent to the sum of the individual responses to fucose and  $\alpha$ -methylaspartate at the same initial concentrations. In comparing the models, we see a larger response for simple additivity due to the inclusion of a response to fucose which was ignored in the other two models. Even with this increase accounting for a response to fucose, the theoretical prediction still falls short of the experimental data. For the antidirectional configuration the response should still be toward the  $\alpha$ -methylaspartate half of the chamber, but with a reduction in peak area related to the fucose peak area for a single stimulus experiment at 0.032 mM. For this configuration the high-sensitivity model more closely represents the experimental data, although based on previous arguments the high-sensitivity model is clearly incorrect.

## Discussion

We first consider the results and analysis of the single stimulus responses to fucose and  $\alpha$ -methylaspartate. The chemotactic sensitivity coefficient for  $\alpha$ -methylaspartate was an order of magnitude greater than the coefficient for fucose. This result is consistent with the general observation that amino acids are stronger attractants than sugars. Koman et al. (1979) noted a seven-fold increase in the response to amino acids over sugars. The analysis by Ford (1992) using the model of Rivero et al. (1989) reported  $\chi_0^{1D}$  values of  $7.5 \times 10^{-4}$  cm<sup>2</sup>/s for  $\alpha$ -methylaspartate and  $8.1 \times 10^{-5}$  cm<sup>2</sup>/s for fucose. A direct comparison of absolute values from this analysis is not possible (due to some of the limitations described in Frymier et al. (1994) of the Rivero et al. model to yield accurate estimates of  $\chi_0$ ). However, it is probable that a more accurate analysis would not alter the conclusion that the value of  $\chi_0$  for  $\alpha$ -methylaspartate is larger by approximately an order of magnitude than the value for fucose. The transport coefficients determined from single stimulus data are qualitatively consistent with the literature and yield bacterial density profiles which characterize our experimental results very well.

Using two amino acids which both evoke strong chemotactic responses may have resulted in more pronounced differences between bacterial density profiles for the co- and antidirectional configurations. Because the response to  $\alpha$ -methylaspartate is much stronger than the response to fucose, using fucose as a second attractant did not have as large an impact on the results as another amino acid may have had.

The differences between the theoretical predictions and the single stimulus experiments at some of the times shown is greater than what would be expected from the standard deviation in the value of  $\chi_0$ . One possible explanation is that the simple equilibrium binding mechanism used to model the signal transduction pathway is not completely accurate. Therefore,

we must exercise some caution in our evaluation of the multiple stimuli data because the single stimulus data are not perfectly matched.

Next we consider the three proposed models for the tumbling probability for multiple stimuli: high-sensitivity, maximum response and simple additivity. The work of Tsang et al. (1973) and Adler and Tso (1974) with attractants and repellents eliminated the dominance of an attractant over a repellent and vice versa. The mere presence of an attractant was not sufficient to overcome the response to a repellent; a gradient in the attractant was required. Our results for two attractants are also consistent with the elimination of the high-sensitivity model. Although this model provides the closest fit to the experimental data for the antidirectional case, it is clear from the experimental data that the presence of the fucose causes a diminished response to the  $\alpha$ -methylaspartate in the antidirectional configuration in comparison to the response in the co-directional configuration. The height of the peak drops from 1.22 to 1.14 in dimensionless units and the area above the trough representing the number of bacteria which responded to  $\alpha$ -methylaspartate is significantly decreased.

Previous work (Adler and Tso, 1974; Pfeffer, 1988; Tsang et al., 1973) with attractants and repellents indicated that the decision to respond to either the attractant or repellent was influenced by the size of the gradient as well as the type of chemoattractant. Our proposed maximum signal model therefore incorporated a measure of the gradient along with the chemotactic sensitivity as the input for the decision to which chemoattractant the bacteria should respond. This model, like the high-sensitivity model, only processes one input, but uses a different criterion for selection. Comparison to experimental data for the multiple attractants shows that this model is no better than the high sensitivity model in representing the data. The apparent conclusion is that bacteria do process both inputs using a common mechanism.

The simplest common mechanism for signal processing is represented by the simple additivity model. The simple additivity model seems closest to what we might expect physically for a receptor-mediated response. It adds together the signals initiated by all the bound receptors. The other two models require the bacteria to somehow distinguish, compare and evaluate several stimuli and then switch off the signal from one or more of them which would be a more complex biochemical process to carry out via a receptor-mediated response. Algebraic additivity of the responses was reported by the previous researchers considering responses to attractants and repellents (Adler and Tso, 1974; Rubik and Koshland, 1978; Tsang et al., 1973). We have represented this in our model by the addition of the chemotactic signal  $\epsilon$  from each of the stimuli as measured in single stimulus experiments. Even this model underestimates the observed experimental data for both co- and antidirectional configurations.

Rubik and Koshland (1978) proposed a response regulator model to account for their observations which seems consistent with the most recent literature regarding the signal transduction mechanism with the level of phosphorylated CheY acting as the regulator. They suggested that such a model would predict different additive properties which could be studied using mutants or multiple stimuli. Their studies with mutants revealed that the bacterial system was capable not only of exact additivity, but also of nonadditivity behaviors such as desensiti-

zation and potentiation observed in higher-order organisms. However, they did not observe potentiation in wild-type cells as we did. One explanation of our experimental data which is consistent with Rubik and Koshland's hypothesis is that the signal from  $\alpha$ -methylaspartate is amplified during the signal processing step. This would explain the result for both configurations. In the co-directional case the response is greater than the model predicts for simple additivity. In the anti-directional case the response is also greater than expected suggesting that the response to methylaspartate is greater in the multiple stimulus case than the single stimulus case alone. A more complex model than any of those presented in this article is required to account for signal being amplified within the cell during processing. In order to develop such a model, we need to understand more about the relationship between the number of bound receptors and the switch activator for the flagellar rotation in order to incorporate a signal amplification model.

## Conclusion

In this article we have presented and analyzed experimental data for single stimulus responses to fucose and  $\alpha$ -methylaspartate to determine transport coefficients. Motility coefficients for the three cell preparations varied from  $(0.88-4.7) \times 10^{-5}$  cm<sup>2</sup>/s and the chemotactic sensitivity coefficients for fucose and  $\alpha$ -methylaspartate were  $(3.9 \pm 0.1) \times 10^{-5}$  cm<sup>2</sup>/s and  $(4.1 \pm 0.2) \times 10^{-4}$  cm<sup>2</sup>/s, respectively. We then proposed hypothetical models (high-sensitivity, maximum signal and simple additivity) for integration of multiple chemoattractants based on observations reported in the literature involving studies of repellents and attractants. These models were based on the use of single stimulus transport coefficients in an approach which can be compared with mixture rules for thermophysical properties. The proposed models for signal processing in the presence of multiple stimuli were incorporated into the cell balance equation for 1-D attractant gradients by modifying the expression for the tumbling probability to account for multiple attractant gradients. The resulting solutions of the cell balance equation were compared with experimentally observed responses to fucose and  $\alpha$ -methylaspartate to co- and antidirectional gradient configurations within the SFDC assay. These results were then used to evaluate the signal processing theories. None of the models accurately predicts the response to multiple attractant gradients observed in our experimental system. We therefore concluded that signal processing involving simple addition of the signals from individual stimuli does not adequately characterize the experimentally observed response to multiple stimuli and suggest that a more complex relationship which accounts for signal processing and amplification is required. This more complex relationship is most likely to be found within the context of a subcellular mechanistic model for signal transduction such as that under development by Bray and co-workers (1993). We are currently investigating the applicability of such a model to multiple stimuli in our laboratory.

## Acknowledgments

Support from the National Science Foundation to RMF through a Research Initiation Award BCS-9109948 is gratefully acknowledged. This research was performed by PDF under appointment to the Environmental Restoration and Waste Management Fellowship Program

administered by Oak Ridge Institute for Science and Education for the U.S. Department of Energy. The IBM Environmental Research Program provided RS/6000 workstations used in computational work associated with this research. Any opinions, findings, and conclusions or recommendations expressed in this material are those of the authors and do not necessarily reflect the views of the IBM Corporation. Helpful comments from Peter Cummings concerning an earlier version of this manuscript are appreciated.

## Literature Cited

- Adler, J., "Chemoreceptors in Bacteria," *Sci.*, **166**, 1588 (1969).
- Adler, J., and M. M. Dahl, "A Method for Measuring the Motility of Bacteria and for Comparing Random and Non-Random Motility," *J. Gen. Microbiol.*, **46**, 161 (1967).
- Adler, J., and B. Templeton, "The Effect of Environmental Conditions on the Motility of *E. coli*," *J. Gen. Microbiol.*, **46**, 175 (1967).
- Adler, J., and W.-W. Tso, "Decision-Making in Bacteria: Chemotactic Response of *Escherichia coli* to Conflicting Stimuli," *Sci.*, **184**, 1292 (1974).
- Alt, W., "Biased Random Walk Models for Chemotaxis and Related Diffusion Approximations," *J. Math. Biol.*, **9**, 147 (1980).
- Armitage, J. P., A. Gallagher, and A. W. B. Johnston, "Comparison of the Chemotactic Behavior of *Rhizobium leguminosarum* With and Without the Nodulation Plasmid," *Mol. Microbiol.*, **2**, 743 (1988).
- Berg, H. C., and D. A. Brown, "Chemotaxis in *Escherichia coli* Analysed by Three-Dimensional Tracking," *Nature*, **239**, 500 (1972).
- Berg, H. C., and L. Turner, "Chemotaxis of Bacteria in Glass-Capillary Arrays," *Biophys. J.*, **58**, 919 (1990).
- Boon, J. P., and B. Herpigny, "Model for Chemotactic Bacterial Bonds," *Bull. Math. Biol.*, **48**, 1 (1986).
- Bosma, T. N. P., J. L. Schnoor, G. Schraa, and A. J. B. Zehnder, "Simulation Model for Biotransformation of Xenobiotics and Chemotaxis in Soil Columns," *J. Contam. Hydrol.*, **2**, 225 (1988).
- Bray, D., R. B. Bourret, and M. I. Simon, "Computer Simulation of the Phosphorylation Cascade Controlling Bacterial Chemotaxis," *Molec. Biol. of the Cell*, **4**, 469 (1993).
- Brown, D. A., and H. C. Berg, "Temporal Stimulation of Chemotaxis in *E. coli*," *Proc. Natl. Acad. Sci. U.S.A.*, **71**, 1388 (1974).
- Chet, I., and R. Mitchell, "Ecological Aspects of Microbial Chemotactic Behavior," *Ann. Rev. Microbiol.*, **30**, 221 (1976).
- Corapcioglu, M. Y., and A. Haridas, "Microbial Transport in Soils and Groundwater: a Numerical Model," *Adv. Water Resour.*, **8**, 188 (1985).
- Dahlquist, F. W., P. Lovely, and J. D. E. Koshland, "Quantitative Analysis of Bacterial Migration in Chemotaxis," *Nature*, **236**, 120 (1972).
- Eisenbach, M., "Signal Transduction in Bacterial Chemotaxis," *Sensory Receptors and Signal Transduction*, J. L. Spudich and B. H. Satir, eds., Wiley-Liss, New York, p. 137 (1991).
- Ford, R. M., "Mathematical Modeling and Quantitative Characterization of Bacterial Motility and Chemotaxis," *Modeling the Metabolic and Physiologic Activities of Microorganisms*, C. J. Hurst, ed., Wiley, New York (1992).
- Ford, R. M., and P. T. Cummings, "On the Relationship Between Cell Balance Equations for Chemotactic Cell Populations," *SIAM J. Appl. Math.*, **52**, 1426 (1992).
- Ford, R. M., and D. A. Lauffenburger, "Analysis of Chemotactic Bacterial Distributions in Population Migration Assays Using a Mathematical Model Applicable to Steep or Shallow Attractant Gradients," *Bull. Math. Biol.*, **53**, 721 (1991a).
- Ford, R. M., and D. A. Lauffenburger, "Measurement of Bacterial Random Motility and Chemotaxis Coefficients: II. Application of Single-Cell-Based Mathematical Model," *Biotechnol. Bioeng.*, **37**, 661 (1991b).
- Ford, R. M., J. A. Quinn, B. R. Phillips, and D. A. Lauffenburger, "Measurement of Bacterial Random Motility and Chemotaxis Coefficients: I. Stopped-Flow Diffusion Chamber Assay," *Biotechnol. Bioeng.*, **37**, 647 (1991).
- Freter, R., B. Allweiss, P. C. M. O'Brien, S. A. Halstead, and M. S. Macsai, "Role of Chemotaxis in the Association of Motile Bacteria with Intestinal Mucosa: In Vitro Studies," *Infect. Immun.*, **34**, 241 (1981).

- Freter, R., P. C. M. O'Brien, and M. S. Macsai, "Effect of Chemotaxis on the Interaction of *Cholera vibrios* with Intestinal Mucosa," *Am. J. Clin. Nutr.*, **332**, 128 (1979).
- Frymier, P. D., R. M. Ford, and P. T. Cummings, "Cellular Dynamics Simulations of Bacterial Chemotaxis," *Chem. Eng. Sci.*, **48**, 687 (1993).
- Frymier, P. D., R. M. Ford, and P. T. Cummings, "Analysis of Bacterial Migration. I. Numerical Solution of Balance Equation," *AIChE J.*, **40**(4), 704 (1994).
- Gristina, A. G., "Biomaterial-Centered Infection: Microbial Adhesion Versus Tissue Integration," *Sci.*, **237**, 1588 (1987).
- Gulash, M., P. Ames, R. C. Larosiliere, and K. Bergman, "Rhizobia are Attracted to Localized Sites on Legume Roots," *Appl. Environ. Microbiol.*, **48**, 149 (1984).
- Harvey, R. W., "Parameters Involved in Modeling Movement of Bacteria in Groundwater," *Modeling the Environmental Fate of Microorganisms*, C. J. Hurst, ed., American Society for Microbiology, Washington, DC, p. 89 (1991).
- Keller, E. F., and L. A. Segel, "Model for Chemotaxis," *J. Theor. Biol.*, **30**, 225 (1971).
- Kennedy, M. J., and J. G. Lawless, "Role of Chemotaxis in the Ecology of Denitrifiers," *Appl. Environ. Microbiol.*, **49**, 109 (1985).
- Koman, A., S. Harayama, and G. L. Hazelbauer, "Relation of Chemotactic Response to the Amount of Receptor: Evidence for Different Efficiencies of Signal Transduction," *J. Bacteriol.*, **138**, 739 (1979).
- Lovely, P. S., and F. W. Dalquist, "Statistical Measures of Bacterial Motility and Chemotaxis," *J. Theor. Biol.*, **50**, 477 (1975).
- Macnab, R. M., and S. I. Aizawa, "Bacterial Motility and the Bacterial Flagellar Motor," *Annu. Rev. Biophys. Bioeng.*, **13**, 51 (1984).
- Macnab, R. M., and D. E. Koshland, "The Gradient-Sensing Mechanism in Bacterial Chemotaxis," *Proc. Natl. Acad. Sci. U.S.A.*, **69**, 2509 (1972).
- Mercer, J. R., R. M. Ford, J. L. Stitz, and C. Bradbeer, "Growth Rate Effects on Fundamental Transport Properties of Bacterial Populations," *Biotechnol. Bioeng.*, **42**, 1277 (1993).
- Mesibov, R., G. Ordal, and J. Adler, "The Range of Attractant Concentrations for Bacterial Chemotaxis and the Threshold and Size of Response Over this Range," *J. Gen. Physiol.*, **23**, 203 (1973).
- Milton, J. S., and J. C. Arnold, *Introduction to Probability and Statistics: Principles and Applications for Engineering and the Computing Sciences*, McGraw-Hill, New York (1990).
- Mowbray, S. L., and J. Koshland D. E., "Additive and Independent Responses in a Single Receptor: Aspartate and Maltose Stimuli on the Tar Protein," *Cell*, **50**, 171 (1987).
- Pfeffer, W., "Über chemotaktische Bewegungen von Bakterien, Flagellaten und Volvocineen," *Untersuch. Bot. Inst. Tübingen*, **2**, 582 (1988).
- Rivero, M. A., R. T. Tranquillo, H. M. Buettner, and D. A. Lauffenburger, "Transport Models for Chemotactic Cell Populations Based on Individual Cell Behavior," *Chem. Eng. Sci.*, **44**, 2881 (1989).
- Rubik, B. A., and D. E. Koshland, "Potentiation, Desensitization and Inversion of Response in Bacterial Sensing of Chemical Stimuli," *Proc. Nat. Acad. Sci. U.S.A.*, **75**, 2820 (1978).
- Sandler, S. I., *Chemical and Engineering Thermodynamics*, Wiley, New York (1977).
- Segel, L. A., "A Theoretical Study of Receptor Mechanisms in Bacterial Chemotaxis," *SIAM J. Appl. Math.*, **32**, 653 (1977).
- Spudich, J. L., and J. Koshland D. E., "Quantitation of the Sensory Response in Bacterial Chemotaxis," *Proc. Nat. Acad. Sci. U.S.A.*, **72**, 710 (1975).
- Staffeld, P. O., D. A. Lauffenburger, and J. A. Quinn, "Mathematical Analysis of Cell Transport Phenomena: Bacterial Chemotaxis in the Capillary Assay," *Chem. Eng. Commun.*, **58**, 339 (1987).
- Stewart, R. C., and F. W. Dahlquist, "Molecular Components of Bacterial Chemotaxis," *Chem. Rev.*, **87**, 997 (1987).
- Stock, J., and A. Stock, "What is the Role of Receptor Methylation in Bacterial Chemotaxis?," *Trends Biochem. Sci.*, **12**, 371 (1987).
- Stock, J. B., A. J. Ninfa, and A. M. Stock, "Protein Phosphorylation and Regulation of Adaptive Responses in Bacteria," *Microbiol. Rev.*, **53**, 450 (1989).
- Strauss, I., "Bacterial Chemotaxis in the Presence of Multiple Stimuli," MS Thesis, Univ. of Virginia (1992).
- Tsang, N., R. Macnab, and J. Koshland D. E., "Common Mechanism for Repellents and Attractants in Bacterial Chemotaxis," *Sci.*, **181**, 60 (1973).

Manuscript received Sept. 9, 1993, and revision received Mar. 21, 1994.